

## SEPARATED FLOWS OVER FINITE-ASPECT-RATIO WINGS: COMPUTATIONAL, EXPERIMENTAL, AND STABILITY ANALYSES

**Kunihiko Taira, Kai Zhang**

Department of Mechanical and Aerospace Engineering  
University of California, Los Angeles, CA, USA  
ktaira@seas.ucla.edu, kzhang3@g.ucla.edu

**Michael Amitay, Shelby Hayostek**

Department of Mechanical, Aeronautical, and Nuclear Engineering  
Rensselaer Polytechnic Institute Troy, NY, USA  
amitam@rpi.edu, hayoss@rpi.edu

**Vassilis Theofilis, Wei He, Anton Burtsev**

School of Engineering  
University of Liverpool, UK  
v.theofilis@liverpool.ac.uk, Wei.He@liverpool.ac.uk, sgaburts@student.liverpool.ac.uk

### ABSTRACT

While the setup of a wing in freestream may appear simple, the flow generated in its wake exhibits complex dynamics. This is especially true for a finite-aspect-ratio wing at a post-stall angle of attack. The wing aspect ratio, angle of attack, sweep angle, wing root condition, and Reynolds number all uniquely contribute to the rich wake dynamics. Although low-aspect-ratio wings are ever more prevalent in aeronautical designs, understanding of these flows is limited due to the vast parameter space. To gain the fundamental insights into low-aspect-ratio wing flows at low Reynolds numbers, we examine the importance of three-dimensional separation and wake behavior. In this paper, we present results of our ongoing endeavor on analyzing separated flows over finite-aspect-ratio wings based on computational, experimental, and theoretical analyses through a collaborative effort by the University of California, Los Angeles (UCLA), the Rensselaer Polytechnic Institute (RPI), and the University of Liverpool (UoL).

### INTRODUCTION

The vast majority of studies of flow separation over airfoils and wings have addressed the 2D limit, in the sense that velocity components along the transverse spatial direction have been considered to be small enough to be ignored. However, flows over finite-aspect-ratio wings exhibit a large-spanwise variation due to the tip effects and the spanwise instabilities that develop in the wake. For translating finite-aspect-ratio wings, the study by Taira & Colonius (2009) reported the 3D nature of the vortical wakes at post-stall conditions. Although the geometry of the wing may be simple, the wake dynamics can exhibit a variety of complex features as summarized by Eldredge & Jones (2019) for a variety of wing maneuvers. The three-dimensionality

of the wake also causes the aerodynamic forces exerted on the wings to depart from their 2D limits, as reported by Torres & Mueller (2004).

For 3D wing configurations, recent studies e.g., Yavuz & Rockwell (2006) have showed that neglecting the spanwise component of velocity is too strong of an approximation, as this component was demonstrated to play a large role in the flow field, as a number of recent studies have shown. In particular, Wygnanski et al. (2011) and (2014) emphatically stressed that the third dimension cannot be ignored in discussion the flow physics of 3D separation. Particularly interesting about a quasi-2D flow is that even where end effects are small, 3D phenomena such as stall cells (Bippes & Turk, 1980) can be present. Weihs and Katz (1983) discovered that there is a relationship between the geometric parameters and the number of cellular shapes that form on a rectangular wing during stall condition. These stall cells can result in loss of lift and other potential detrimental effects. Recently, Dell'Orso & Amitay (2018) mapped out the flow regime at Reynolds number of  $O(10^5 - 10^6)$  where these stall cells occur.

Rodríguez & Theofilis (2011) observed stall cells arising from linear instability of a 3D (spanwise periodic) self-excited global mode on a stalled symmetric airfoil at  $Re = 200$ . More recent modal and non-modal instability analysis (He *et al.*, 2017a) has refined these predictions and showed that the stationary 3D mode reported by Rodríguez & Theofilis (2011) is more amplified than the 3D Kelvin-Helmholtz (KH) instability only at small spanwise periodicity lengths  $L_z$  (concretely, at  $\beta = 2\pi/L_z > 3$ ), while for large  $L_z$  ( $0 < \beta < 3$ ) the KH mode is the dominant global flow instability. This result holds at all three airfoils examined by He *et al.* (2017a), independently of thickness and camber, and all angles of attack. The implication is that the wake behind stalled airfoils at low Reynolds numbers first becomes

unsteady due to linear amplification of the KH mode, followed by 3D secondary (Floquet) instability that has been documented by He *et al.* (2017a) to peak around  $\beta = 11$  at all Reynolds number values examined, up to  $Re = 600$ .

Questions left open in the above studies mainly concern the physical mechanisms by which finite-wing-geometry affects the flow separation and the wake formation at moderate to high angles of attack. We are in particular interested in the genesis of flow structures that persist at flight Reynolds numbers and thus examine the influence of aspect-ratio, sweep angle, Reynolds number, angle of attack, and the root plane boundary condition on such structures. The present effort addresses these questions in a three-pronged collaborative research effort: computational (UCLA), experimental (RPI), and stability (UoL) analyses. The findings from each group are combined to take advantage of the strengths from each of the efforts and complement each components of the overall research endeavor. Below, we describe the approach taken, present some research highlights, and offer some concluding remarks.

## PROBLEM SETUP AND APPROACHES

In this study, we study the separated flows behind finite-aspect-ratio wings with a cross section of NACA0015 airfoil in pure translation. In order to gain fundamental knowledge into the wake dynamics, we consider the flows in the laminar regime. The chord-based Reynolds number is  $Re = 400$  to  $600$ , since experiments and numerical simulations performed in the framework of this effort have verified that qualitative changes exist in flows in the above Reynolds number range, or at  $Re = 1000$  and above. To examine the influence of tip effects on the three-dimensional flow separation and wake dynamics, we consider wings over a range of aspect ratios. The aspect ratio is reported as  $AR = b/c$ , where  $b$  is the span and  $c$  is the chord length. Different boundary conditions, namely the symmetry, no-slip wall and free end conditions, have been used at the root of the wing. Unless otherwise stated, the aspect ratios reported within this work are all based on the actual span in the numerical or experimental setup.

## Numerical simulations

In the computational component of the work, we numerically solve the three-dimensional Navier-Stokes equations to investigate the wake dynamics behind the finite-aspect-ratio wings. The direct numerical simulations are carried out with the incompressible flow solver *Cliff* (included in the *CharLES* software package, Cascade Technologies, Inc), which employs the finite-volume formulation with second-order accuracy in time and space (Ham & Iaccarino, 2004; Ham *et al.*, 2006).

## Experiments

The experiments are conducted in a closed return, closed test section water tunnel downstream of finite span, cantilevered or free ends NACA 0015 airfoils by the use of stereo-particle velocimetry (*SPIV*). For the free ends model, the airfoils have to be mounted away from the wall, outside of the boundary layer effect by the use of a single thin rod at one end of the airfoil. The flow fields are captured using a LaVision *SPIV* system with a dual Nd:YAG laser with a maximum output of 120 mJ/pulse and two 2 Megapixel ImagerPro X CCD cameras. A laser sheet is

emitted through the tunnel floor to collect data in multiple streamwise planes, which are 1 mm apart. At each plane 500 image pairs are collected, averaged and then combined to form a time-averaged flow volume.

## Stability analysis

The 3D nature of the problem, in which no homogeneous spatial direction is assumed, implies the need to perform TriGlobal linear stability analysis (Theofilis, 2003). The incompressible Navier-Stokes and continuity equations are linearised by decomposing the velocity and pressure components into a base flow and a superposed small-amplitude perturbation. The numerical work, of which here only modal stability analysis results are shown, has been performed in the framework of the *hp*-spectral element open-source code Nektar++ (Cantwell *et al.*, 2015). Base flows around 3D finite aspect ratio wings with a mid-span symmetry boundary condition are computed on a structured C-type grid. For naturally unstable flows, such as those occurring at high angles of attack, selective frequency damping (SFD) (Åkervik *et al.*, 2006) is used to construct the steady base flow, that could subsequently be interrogated as regards its linear modal instability.

## RESULTS

### Unswep wings

The wake structures behind the unswept wing obtained from DNS with the symmetry boundary condition at the mid-span are shown in figure 1 for the cases of  $(\alpha, AR, Re) = (22^\circ, 1 - 6, 400)$ . As it can be clearly seen, the wake exhibits strong three-dimensionality over the entire flow field. The wake structures are comprised of different vortical features. The tip vortex remains steady over time (except for  $AR = 1$ ) with the unsteady shedding vortices influenced by the aspect ratios. At small aspect ratio of 2, vortex cores with  $\omega_x$  and  $\omega_y$  shed periodically from the wing into the wake. With the increase of aspect ratio, long spanwise vortices become prominent. Above  $AR = 6$ , vortex dislocation occurs, dividing the spanwise shedding region into two cells. This phenomenon has also been observed in general bluff body flows with inhomogeneous boundary conditions (Williamson, 1989; Noack *et al.*, 1991).

Figure 2 shows the most unstable global eigenmode in the wake of an aspect ratio 4 wing at  $Re = 400$  and angle of attack of  $22^\circ$ . The three-component normalized vorticity amplitude function is visualized at  $\hat{\omega} \in [-0.1, 0.1]$ . It can be seen that the dominant structure is associated with the wake region close to the symmetry plane. This structure is interpreted as two parallel branches, both of which are akin to Kelvin-Helmholtz instability, a result that is reminiscent of the analogous findings of He *et al.* (2017b) in the wake of an elliptic wing. Interestingly, in the elliptic wing case cuts through the amplitude function of the three-dimensional global mode, made perpendicularly to the mean flow direction at arbitrary locations in the wake, matched closely the amplitude functions delivered by classic linear local (spatial) instability analysis based on numerical solution of the Orr-Sommerfeld equation. The region that exhibits instability and the region that exhibits the highest level of unsteadiness based on DNS are in agreement. There are ongoing efforts to further examine the correlation between the findings from simulations/experiments and the global stability analysis.

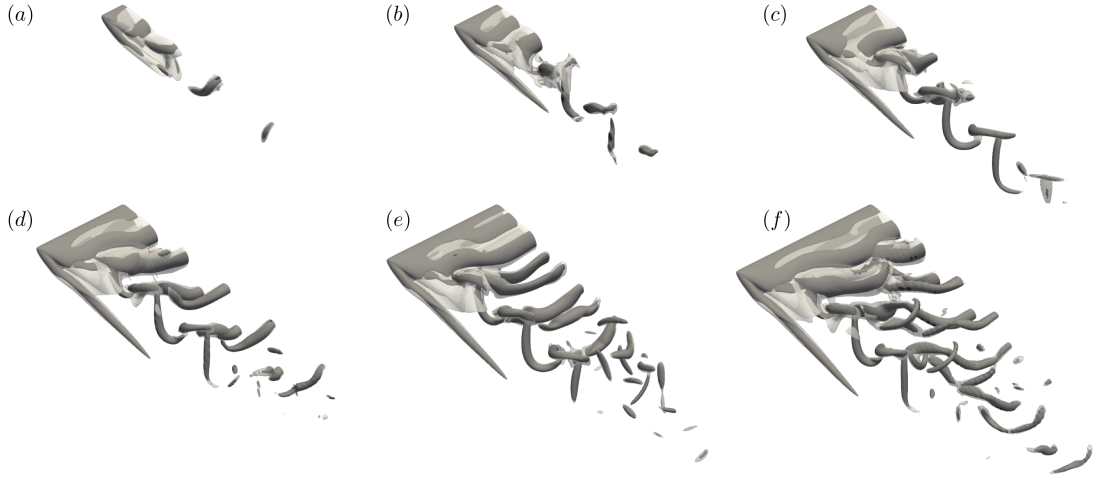


Figure 1: Vortical structures visualized by  $Q = 1$  (transparent) and  $Q = 2$  (green) behind an unswept wings with different aspect ratios. Shown are the cases  $(\alpha, Re) = (22^\circ, 400)$ . (a) – (f):  $AR = 1, 2, 3, 4, 5$  and  $6$ . Symmetry boundary condition is prescribed at the mid-span for the current cases.

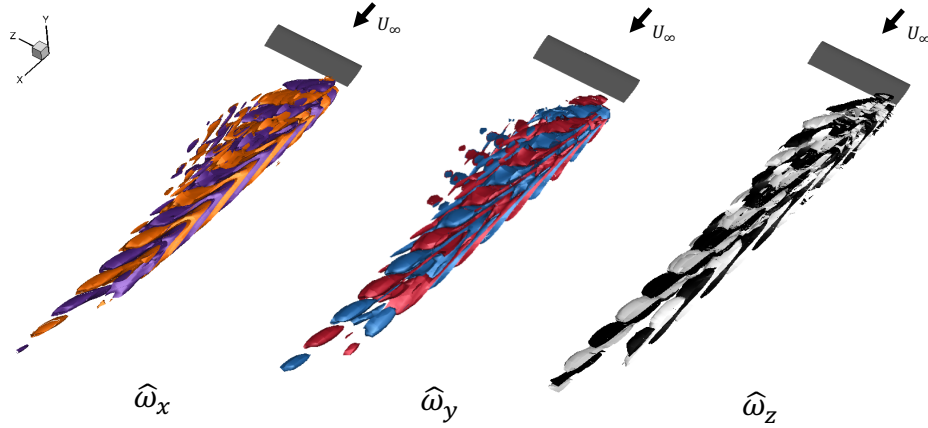


Figure 2: The most unstable mode of finite wing  $(\alpha, AR, Re) = (22^\circ, 4, 400)$  with midspan symmetry boundary condition. Visualized by three-component vorticity. The symmetry plane is at right.

The influence of the mid-span boundary condition is also being considered in this work. With the prescription of the no-slip boundary condition (representative of the experimental setup), the wake dynamics is altered. The least stable TriGlobal mode from stability analysis that corresponds to the full water tunnel case  $(\alpha, AR, Re) = (20^\circ, 6, 600)$  is shown in Figure 3. In qualitative analogy to the mid-span symmetry configuration the dominant mode of the full tunnel setup is associated with the wake region.

### Swept wings

As discussed above, the wakes behind unswept wings possess complex dynamics. The nature of the dynamics is significantly altered for swept wings. We compare the wake flow behind a wall-mounted wing obtained in water tunnel experiment as shown in figure 4. For the experiments, there is a no-slip wall at the root with a formed boundary layer (figure 4(top)). In the simulations, we prescribe the symmetry boundary condition at the mid-span (figure 4(bottom)). Despite the difference in the boundary conditions, these two cases show great similarity in terms of the strong axial flow in the near wake. Such spanwise flow alters the wake in a drastic manner, compared to those seen in figure 1.

The added richness of the wake dynamics from sweep

is summarized in figure 5 based on DNS results in which mid-span symmetry has been imposed. The vortical structures are visualized for the cases of  $(\alpha, AR, Re, \Lambda) = (22^\circ, 4, 400, 7.5^\circ - 45^\circ)$ . For  $\Lambda = 7.5^\circ$ , the wake behind the swept wing consists of the tip vortex at the free end and the periodically shedding vortices near the mid-span. Such wake structures resemble that of the unswept cases shown in figure 1. Increasing the sweep angle to  $15^\circ$ , leads to the formation of a steady wake near the mid-span region. The unsteady shedding vortices are pushed towards the wing tip, breaking down the originally steady tip vortex. With a further increase of  $\Lambda$ , the whole flow field becomes steady, and the tip vortex disappear. The wake is characterized by spiky vortical structures trailing into the wake. It is indeed remarkable that an increase of the sweep angle offers a stabilizing effect to the flow field in terms of a reduction the region of instability. While the quantification of the causal relationship between sweep angle and flow instability is currently underway, our work clearly shows that at high sweeps the flow at this Reynolds number loses the spanwise shedding instabilities.

We further note that the mid-span boundary condition plays an important role in determining the wake dynamics. As an illustration, we present experimental and computa-

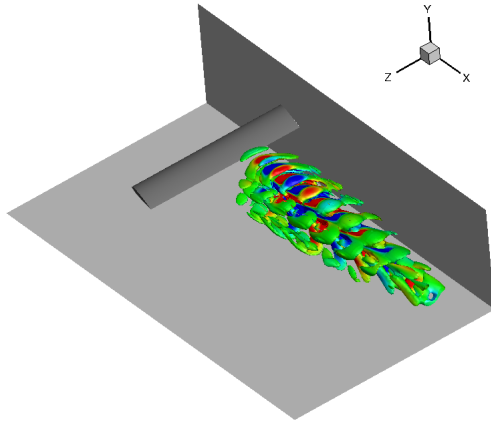


Figure 3: The most unstable TriGlobal mode for the full water tunnel configuration  $(\alpha, AR, Re) = (20^\circ, 6, 600)$  visualized by  $Q = 0.001$  and coloured by the streamwise velocity  $\hat{u}$ .

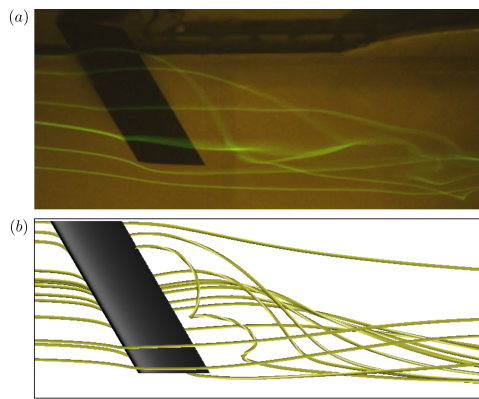


Figure 4: (a): Dye flow visualization for the case  $(\alpha, AR, Re, \Lambda) = (22^\circ, 2, 600, 30^\circ)$ . (b): Streamline from CFD for the case  $(\alpha, AR, Re, \Lambda) = (20^\circ, 2, 600, 30^\circ)$ . Note that in the experimental setup, no-slip wall is used at the root, whereas the computational setup employs the symmetry boundary condition at the mid-span.

tional results of the flow field for a wing with two free ends, as visualized in figure 6. In both of these results strong agreement of the respective wake structures can be seen, accompanied by a family of streamwise vortices in formation. A distinct tip vortex is also observed at one end of the airfoil that is colored by positive vorticity with a counter-clockwise rotation. However, due to the sweep, the rest of the vortical structures are pushed outboard, toward the left side of the image. Due to the interaction of the vortices with the spanwise velocity and among themselves, they are less coherent.

## CONCLUDING REMARKS

We have presented our collaborative efforts on revealing the physics of 3D separated flows past finite-aspect-ratio wings in uniform translation. The computational, experiment, and stability analyses are performed in a complementary manner aiming at uncovering physical mechanisms

governing the complex wake dynamics. The results presented herein showed that each component of the efforts is in agreement with one another and highlights each of their strengths to understand the detailed physics over a vast parameter space comprised of wing aspect ratio, angle of attack, sweep angle, Reynolds number, and root boundary condition. All of these parameters are found to have significant influence on the wake dynamics in unique ways.

There is a range of ongoing work with this project. In addition to exploring the boundaries of this multi-parametric problem, two major thrusts are pursued. First is to analyze the implications of instabilities in the wake formation and separation. Preliminary results show that global instabilities can provide guidance on the emergence of surface separation patterns, as shown in figure 7. Second is to examine the full wing geometries, while allowing spanwise motion across the midspan. As shown in figure 8, such configurations are inspired by 3D wing configurations akin to those found on air vehicles.

Finally, it should be noted that in all configurations studied in the present work have considered wakes that are symmetric with respect to the mid-span plane, in both unswept and swept wings. Such symmetry is expected to break down at higher Reynolds number or angles of attack, as reported by Taira & Colonius (2009). Efforts in this direction are also underway and will be reported in future work.

## ACKNOWLEDGEMENTS

This work was supported by the AFOSR (grant number: FA9550-17-1-0222) monitored by Drs. Douglas Smith and Gregg Abate. The authors also acknowledge the support of the National Science Foundation for funding SH. This material is based upon work partially supported by the National Science Foundation under Grant No. DGE-1744655. Any opinions, findings, and conclusions or recommendations expressed in this material are those of the authors and do not necessarily reflect the views of the National Science Foundation.

## REFERENCES

- Åkervik, E., Brandt, L., Henningson, D. S., Høpfner, J., Marxen, O. & Schlatter, P. 2006 Steady solutions of the Navier-Stokes equations by selective frequency damping. *Phys. Fluids* **18**, 068102.
- Bippes, H. & Turk, M. 1980 Windkanalmessungen an einem Rechteckflügel bei anliegender und abgelöster Strömung (wind tunnel measurements on a rectangular wing in attached and separated flow). *Tech. Rep.*. DFVLR IB-251-80-A18 (West Germany).
- Cantwell, C.D., Moxey, D., Comerford, A., Bolis, A., Rocco, G., Mengaldo, G., Grazia, D. De, Yakovlev, S., Lombard, J.E., Ekelschot, D., Jordi, B., Xu, H., Mohamied, Y., Eskilsson, C., Nelson, B., Vos, P., Biotto, C., Kirby, R.M. & Sherwin, S.J. 2015 Nektar++: an open-source spectral/hp element framework. *Comput. Phys. Commun.* **192**, 205–219.
- Dell'Orso, H. & Amitay, M. 2018 Parametric investigation of stall cell formation on a naca0015 airfoil. *accepted to AIAA Journal*.
- Eldredge, Jeff D & Jones, Anya R 2019 Leading-edge vortices: mechanics and modeling. *Annual Review of Fluid Mechanics* **51**, 75–104.

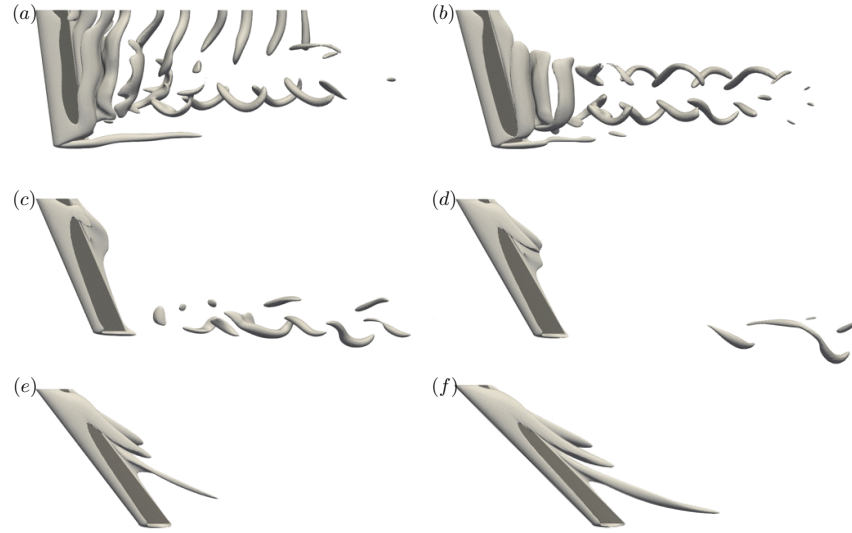


Figure 5: Vortical structures of flow behind swept wings with  $AR = 4$ ,  $\alpha = 20^\circ$  and  $Re = 400$ . (a) – (f):  $\Lambda = 7.5^\circ$ ,  $15^\circ$ ,  $22.5^\circ$ ,  $30^\circ$ ,  $37.5^\circ$  and  $45^\circ$ . Shown are iso-surfaces of  $Q = 1$ .

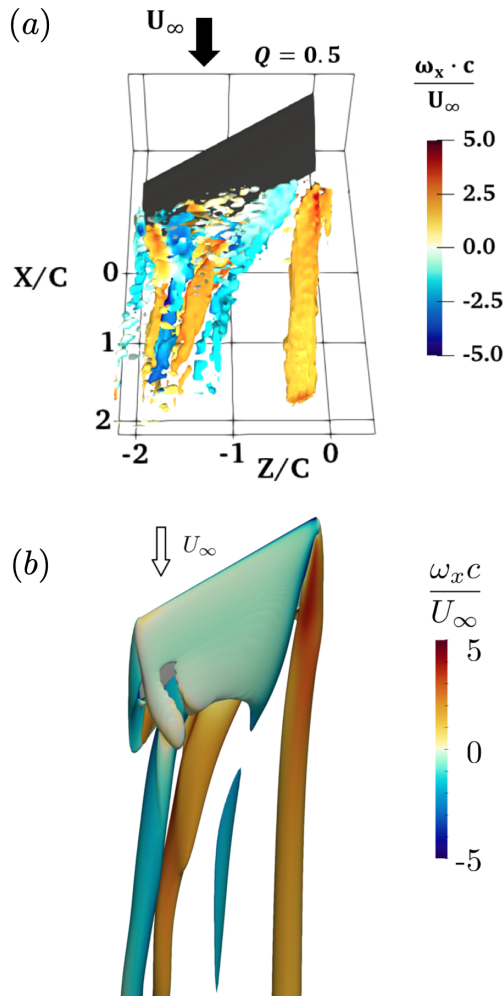


Figure 6: Wake behind a swept finite wing with two free ends. (a) Experimental result and (b) numerical result. In both cases, the case of  $(\alpha, AR, Re, \Lambda) = (22^\circ, 2, 600, 30^\circ)$  is studied. Iso-surfaces of  $Q = 0.5$  are colored by streamwise vorticity.

- Ham, F. & Iaccarino, G. 2004 Energy conservation in collocated discretization schemes on unstructured meshes. *Annual Research Briefs, Center for Turbulence Research* **2004**, 3–14.
- Ham, F., Mattsson, K. & Iaccarino, G. 2006 Accurate and stable finite volume operators for unstructured flow solvers. *Annual Research Briefs, Center for Turbulence Research* pp. 243–261.
- He, W., Gioria, R., Pérez, J. M. & Theofilis, V. 2017a Linear instability of low Reynolds number massively separated flow around three naca airfoils. *Journal of Fluid Mechanics* **811**, 701–741.
- He, W., Tendero, J. A., Paredes, P. & Theofilis, V. 2017b Linear instability in the wake of an elliptic wing. *Theoretical and Computational Fluid Dynamics* **31**, 483–504.
- Noack, B. R., Ohle, F. & Eckelmann, H. 1991 On cell formation in vortex streets. *J. Fluid Mech.* **227**, 293–308.
- Rodríguez, D. & Theofilis, V. 2011 On the birth of stall cells on airfoils. *Theoretical and Computational Fluid Dynamics* **25**, no. 1-4, 105–117.
- Taira, Kunihiko & Colonius, TIM 2009 Three-dimensional flows around low-aspect-ratio flat-plate wings at low Reynolds numbers. *Journal of Fluid Mechanics* **623**, 187–207.
- Theofilis, V. 2003 Advances in global linear instability of nonparallel and three-dimensional flows. *Prog. Aerosp. Sci.* **39** (4), 249–315.
- Torres, G.E. & Mueller, T.J. 2004 Low-aspect-ratio wing aerodynamics at low Reynolds number. *AIAA Journal* **42** (5), 865–873.
- Weihls, D. & Katz, J. 1983 Cellular patterns in poststall flow over unswept wings. *AIAA* **21**, no. 12, 1757–1759.
- Williamson, C. H. K. 1989 Oblique and parallel modes of vortex shedding in the wake of a circular cylinder at low Reynolds numbers. *J. Fluid Mech.* **206**, 579–627.
- Wynanski, I., Tewes, P., Kurz, H., Taubert, L. & Chen, C. 2011 The application of boundary layer independence principle to three-dimensional turbulent mixing layer. *Journal of Fluid Mechanics* **675**, 336–346.
- Wynanski, I., Tewes, P., Kurz, H., Taubert, L. & Chen, C.



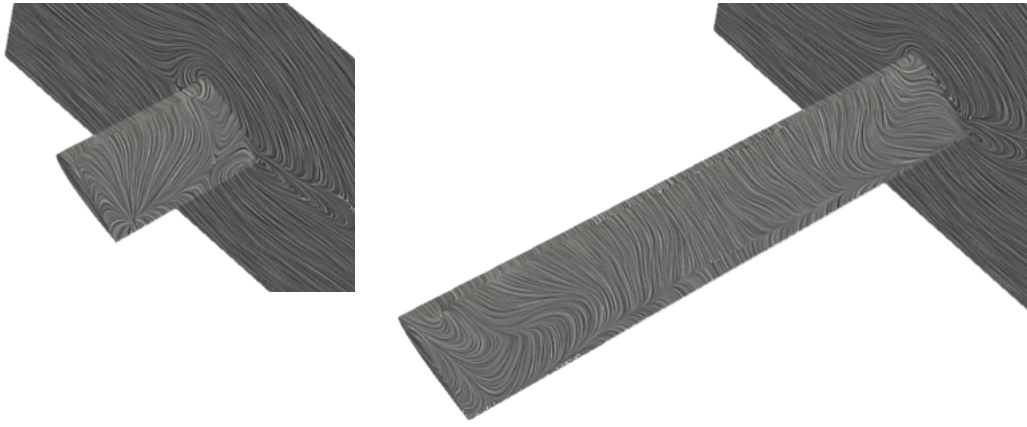


Figure 7: Dominant surface streamline patterns from leading global instabilities.

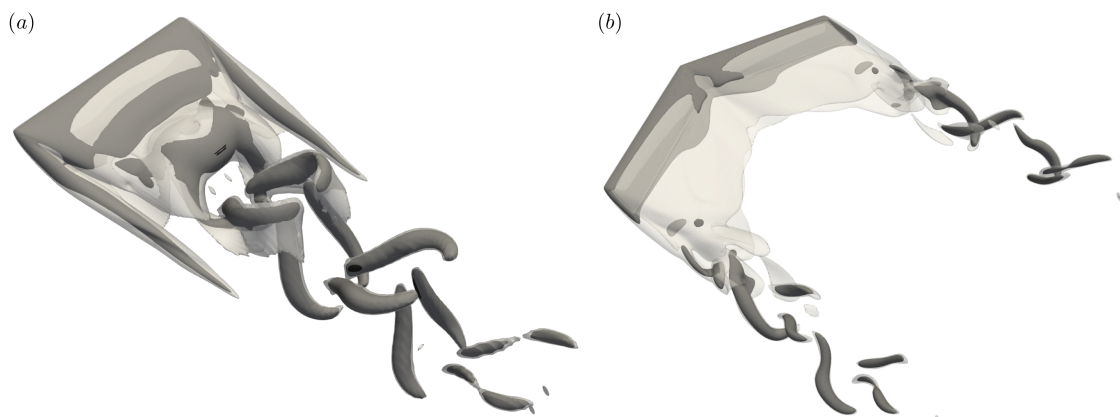


Figure 8: Wake structure behind full wing models. (a) An unswept wing with  $(\alpha, AR, Re) = (22^\circ, 4, 400)$  and (b) a swept wing with  $(\alpha, AR, Re) = (20^\circ, 8, 400)$ . Iso-surfaces of  $Q = 1$  are shown in darker gray and  $|\omega| = 2$  in transparent.

2014 Applying the boundary-layer independence principle to turbulent flows. *Journal of Aircraft* **51**, no. 1, 336–346.  
 Yavuz, M. M. & Rockwell, D. 2006 Identificaiton and con-

trol of three-dimensional separation on low swept delta wing. *AIAA J.* **44**(11), 2805–2811.